ISSN 1063-7710, Acoustical Physics, 2015, Vol. 61, No. 2, pp. 181–187. © Pleiades Publishing, Ltd., 2015.
Original Russian Text © O.A. Sapozhnikov, M.A. Smagin, 2015, published in Akusticheskii Zhurnal, 2015, Vol. 61, No. 2, pp. 199–206.

PHYSICAL ACOUSTICS

Finding the Dispersion Relations for Lamb-Type Waves in a Concave Piezoelectric Plate by Optical Visualization of the Ultrasound Field Radiated into a Fluid

O. A. Sapozhnikov[a, b] and M. A. Smagin[a]

[a] *Physics Faculty, Department of Acoustics, Moscow State University, Moscow, 119991 Russia*
[b] *Center for Industrial and Medical Ultrasound, Applied Physics Laboratory, University of Washington, 1013 NE 40th Street, Seattle, WA 98105, USA*
e-mail: oleg@acs366.phys.msu.ru

Received July 8, 2014

Abstract—We propose and experimentally demonstrate a method for measuring the phase velocities of Lamb waves in concave piezoelectric plates submerged in a fluid. The method is based on the optical shadowgraphy method of visualizing the ultrasound field that occurs in a fluid when Lamb modes are excited in the plate under study. According to the condition of wave resonance, the propagation direction of the waves radiated into the fluid is determined by the phase velocity of a Lamb wave in the plate, which makes it possible to measure the indicated velocity. Proceeding from this, we demonstrate that when spherical concave piezoelectric plates are used, the phase velocities of Lamb waves can be determined by the position of the caustics—areas of acoustic wave focusing in the fluid. We have experimentally measured the dispersion curves of several Lamb modes for a concave piezoelectric plate with a diameter of 100 mm and thickness of around 2 mm, which was submerged in water. Ultrasound waves were optically visualized in the fluid by the schlieren method on a specially designed setup, in which off-axis parabolic mirrors were used to implement the dark-field method. We demonstrated that the measured dispersion curves for low-order Lamb modes are well described by the theoretical dependences calculated using the Rayleigh–Lamb equation.

Keywords: Lamb waves, piezoelectric plate, ultrasound transducer, optical shadowgraphy method, schlieren visualization

DOI: 10.1134/S106377101501011X

INTRODUCTION

Lamb waves are normal modes that occur during propagation of elastic perturbations in a solid plane-parallel plate with mechanically free sides [1, 2]. Particle displacement of the medium under the action of a wave occurs in the plane formed by the direction of wave propagation and the normal to the plate.

Although Lamb waves are the solution to the wave problem in perfect conditions (the plate is assumed to be plane-parallel and bordered by a vacuum on both sides), the main features of the propagation of elastic perturbations are well described by the Lamb theory in real conditions as well. Thus, in practice, plates are usually not located in a vacuum, but are surrounded by an acoustically soft medium—a gas or liquid. Owing to this, Lamb waves become "leaky waves" [3], since during their propagation they lose energy to radiation into the medium. However, the corresponding attenuation is usually small; therefore, the properties of normal waves remain close to those of Lamb modes [4, 5]. Moreover, such attenuation can be beneficial. An acoustic signal occurring in an immersion medium due to the mentioned leakage carries information on the velocity and attenuation of the plate wave generating that signal. It thereby becomes possible to remotely measure the properties of Lamb waves. In this work, such an approach was used to study Lamb-type waves in a piezoelectric plate bordered by a fluid. A similar situation is common for ultrasound transducers used in hydroacoustics, medicine, and nondestructive testing.

The Lamb waves that occur during the operation of piezoelectric sources are a "parasitic" effect with respect to the thickness mode of plate vibrations [6–10]. These additional waves are excited in places where the plate is fixed on the transducer casing at a place where the homogeneity conditions are violated. Usually, this is the plate edge. Owing to excitation of Lamb waves, the character of surface vibrations of piezoelectric radiators is nonuniform, which is important to take into account in applications [11]. Figure 1 shows a typical distribution of the normal component of the vibration velocity on the surface of a flat circular piezoelectric plate submerged in water and excited at a frequency close to that of mechanical resonance. The distribution is obtained by acoustic holography, described in [12]. In the 2-D picture (Fig. 1a), one can

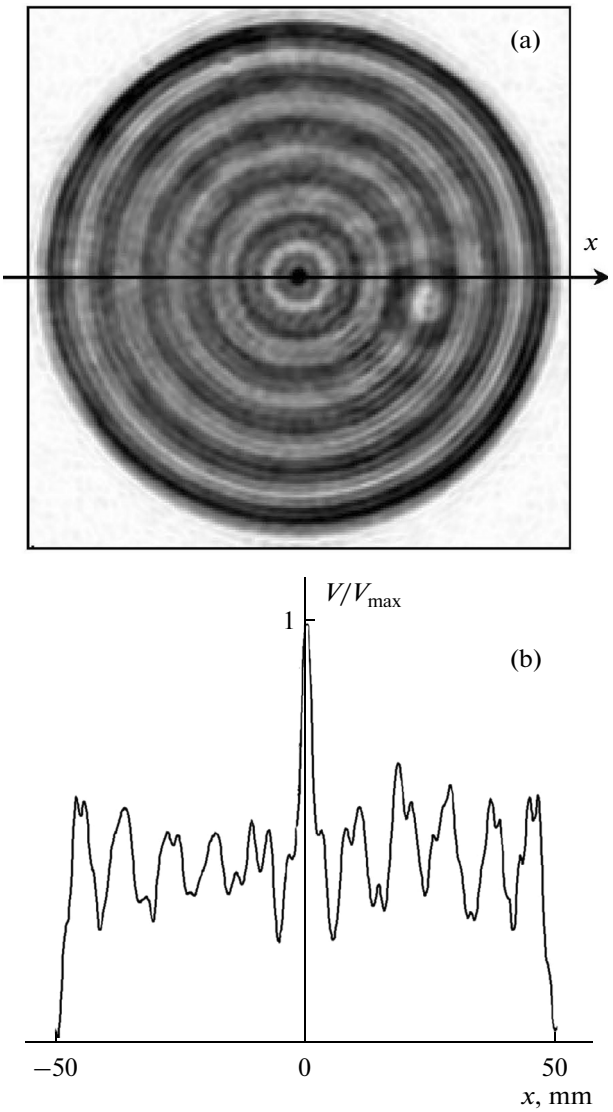

Fig. 1. Characteristic view of distribution of normal components of vibration velocity on piezoelectric transducer surface. Velocity distribution for a flat circular piezoceramic source with diameter of 100 mm during its excitation at frequency of 1.14 MHz. (a) Two-dimensional amplitude distribution of normal velocity component along surface. (b) Dependence of velocity amplitude along axis passing through center of plate (axis *Ox*). Velocity normalized to its maximum value. Distribution obtained experimentally by acoustic holography. Structure of standing waves caused by Lamb wave interference is distinctly seen.

distinctly see an annular structure with two periodicity scales in it, which indicate the excitation of two Lamb modes. The amplitude distribution of the vibration velocity along the diameter shows that surface vibration is strongly inhomogeneous; i.e., the contribution of Lamb modes to surface vibrations of the piezoelectric plate is comparable to the contribution of the thickness mode of vibrations (Fig. 1b).

When elastic waves propagate in piezoelectric plates, a certain specificity occurs. First, the plate material cannot be considered isotropic [13]. Second, mechanical deformations are accompanied by excitement of an electric field, the character of which is determined by the presence of metallization on the plate faces and the electric load conditions of the transducer. Although these factors somewhat complicate theoretical analysis of waves in a plate, the corresponding waves are nevertheless close to classical Lamb waves in their properties. Note also that along with Lamb waves in plates, waves of another type can be excited [14], but they play no role in the processes studied here.

One of the convenient methods for studying acoustic waves in optically transparent media is the shadowgraphy method, which is based on the fact that acoustic perturbations in the density of a medium lead to corresponding changes in the refractive index of light [15]. The shadowgraphy method is widely used in ultrasound studies, since it allows real-time visualization of acoustic fields in a large volume. Bergmann presents many interesting examples of such visualization in his monograph [16]. In particular, it is possible to record waves radiated into a fluid by oscillating shells using such a method [17, 18]. Such an approach is used in this work to study Lamb-type leaky waves.

EXPERIMENTAL

Lamb waves are excited in a piezoelectric plate polarized in thickness and having the shape of a spherical cup. As is usually done in piezoelectric transducers, opposing plate surfaces were metalized (covered with a thin silver layer). The plate material was a C5400 PZT piezoceramic (Channel Industries, Santa Barbara, CA, United States). The geometric dimensions of the piezoelectric plate were as follows: thickness 2.15 mm, diameter 100 mm, curvature radius of the concave side 92.1 mm. The plate was fixed along the perimeter in a hermetic stainless steel casing. An external generator fed electric voltage to the opposite side of the plate via a high-frequency cable. The concave side of the piezoelectric plate was turned outward. The structure obtained as a result was a focused ultrasound transducer with an air backing. Figure 2 shows an external view.

The acoustic parameters of the piezoceramics were known only approximately; therefore, they were refined in the course of work. In particular, by measuring the frequency dependence of the electric impedance of the transducer, we determined the frequency of the main thickness resonance, $f_0 = 1.08$ MHz. Taking into account the fact that $f_0 = c_l/(2h)$, from the found value of the resonance frequency and the known thickness of the plate $h = 2.15$ mm, we obtain the value of the velocity of longitudinal waves in the piezoceramic, $c_l = 4.64$ mm/μs.

The edge of the piezoceramic plate was the source of the Lamb waves under study: at the edge, the homogeneity conditions were inevitably violated both for

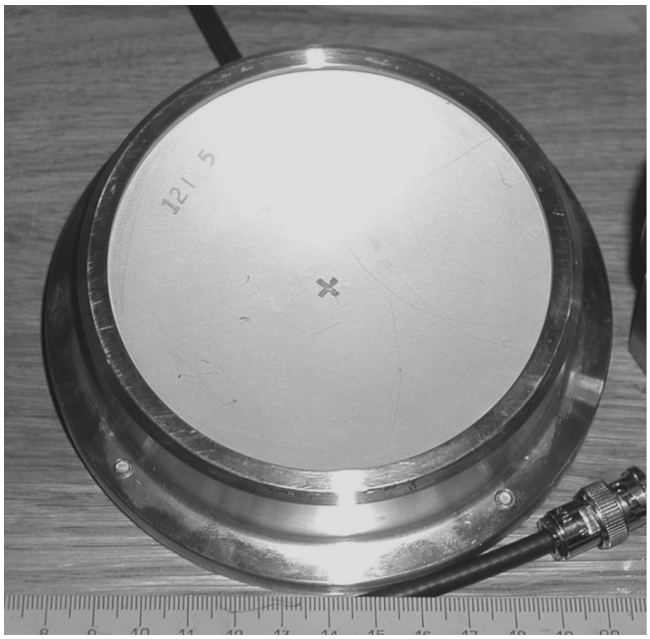

Fig. 2. Photograph of studied piezoelectric transducer.

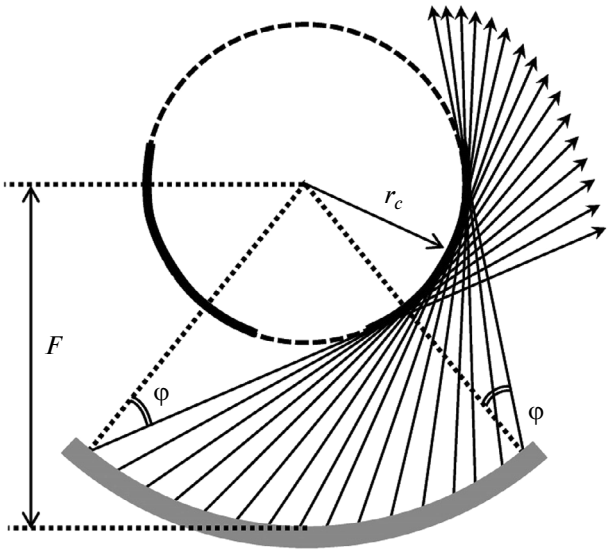

Fig. 3. Formation of caustics during ultrasound radiation by spherically concave plate in which Lamb waves propagate.

mechanical motion and the electric field; therefore, the thickness character of plate vibrations was perturbed. These perturbations propagated in the form of different Lamb modes toward the center of the cup, losing energy to acoustic radiation into the fluid as they propagated. Then, the Lamb waves reached the center of the plate and transformed to diverging waves, as a result of which, the resulting distribution of elastic deformations in the plate assumed the character of a standing wave. Note that due to leakage, Lamb perturbations noticeably attenuated already after the first re-reflection; therefore, the corresponding radial resonances were strongly suppressed—i.e., the influence of Lamb waves on the inhomogeneous character of surface vibration was approximately identical at all frequencies. The noted regularities for a similar piezoelectric radiator were revealed with a laser vibrometer [9].

It should be mentioned that owing to the curvature of the studied piezoceramic plate, propagation of elastic waves in it, strictly speaking, somewhat differ from propagation in a plane-parallel layer. However, in the described experiment, it was possible to ignore the influence of plate curvature on the character of generated modes, since the curvature was very weak: the surface curvature radius (F = 92.1 mm) exceeded the thickness of the plate by many times (h = 2.15 mm).

The curved shape of the plate has certain advantages when experimentally studying ultrasound fields radiating into the surrounding fluid during propagation of Lamb waves in a plate. Owing to the concavity of the radiating surface, a convenient focusing effect is achieved. The occurring high-intensity ultrasound zones correspond to the caustics, which can be calculated in the geometric acoustics approximation. According to this notion, points of the radiated surface emit ultrasound rays to the fluid. The direction of rays is found from the condition that the velocity of the trace of an outgoing quasi-plane wave $V = c_0/\sin\varphi$ coincides with the phase velocity c_{ph} of the corresponding wave in the plate:

$$c_0/\sin\varphi = c_{\text{ph}}, \tag{1}$$

where φ is the angle between the normal to the plate and the direction of the ultrasound wave departing from it, and c_0 is the sound velocity in a fluid. The caustics in this case will be the envelope of the family of rays emitted into the fluid from the surface of the cup as Lamb waves propagate in it. According to condition (1), each ray is emitted at an angle of $\varphi = \arcsin\left(c_0/c_{\text{ph}}\right)$ to the normal to the plate. If the emitting surface is spherical, like in the case under study, then the corresponding caustic surface is also spherical and these two spheres are concentric. Figure 3 schematically shows the corresponding ray pattern and location of the caustics. From the location of the rays, one can easily see that the radius of the sphere to which the caustics belongs is $r_c = F\sin\varphi = F\cdot c_0/c_{\text{ph}}$. This relation makes it possible to calculate the phase velocity of a wave in the plate from measurements of distance r_c from the center of the plate curvature to the caustics for known values of F and c_0 [18]:

$$c_{\text{ph}} = c_0\cdot F/r_c. \tag{2}$$

The accuracy of finding velocity c_{ph} is determined by the error in measuring quantity r_c, which mainly results from diffraction smearing of the ultrasound field in the region of the caustics.

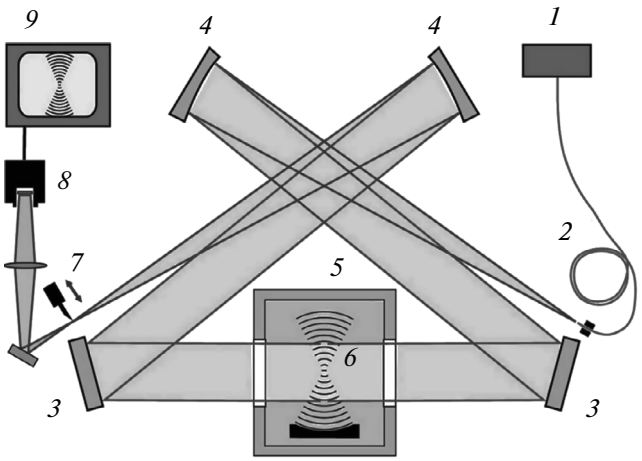

Fig. 4. Diagram of setup for optical visualization of ultrasound acoustic fields. *1*, light source; *2*, optical fiber; *3*, flat mirrors; *4*, off-axis parabolic mirrors; *5*, water tank; *6*, studied acoustic field; *7*, optical knife; *8*, digital camera.

During the experiments, the studied ultrasound transducer was in a water-filled tank with optically transparent sides. The transducer was excited by a harmonic signal at a given frequency from an HP33120A generator and an ENI AP400B broadband electric amplifier. The velocity of Lamb waves was determined by formula (2), the quantity r_c in which was found by the optical shadowgraphy method (see below) at different frequencies in the range from 300 kHz to 1.5 MHz. The level of electric voltage fed to the transducer was selected for each frequency such that the power of the ultrasound beam emitted into the fluid was sufficient for the occurrence of a distinct shadow pattern. For each measurement, the shadow pattern was recorded after 200 vibration periods after onset of excitation of the transducer at the assigned frequency. Analysis of transients showed that for the indicated lag, the acoustic field in the fluid entered a steady state mode until distortions occurred due to reflection of ultrasound from the walls of the tank.

The shadow patterns were observed with a specially designed optical schlieren visualization system (Fig. 4). In this system, the light source was a semiconductor laser with radiation wavelength of 670 nm and a mean power of 10 mW ("Polyus" Research Institute, Moscow). The laser radiation was controlled by triggering-and-illumination block *1*, which made it possible to generate laser pulses of up to 10 ns in duration at an arbitrary repetition rate; it was also possible to synchronize radiation of laser pulses with the electric generator that powered the studied ultrasound transducer. In addition to the pulse mode, the block controlling laser illumination was able to operate in the continuous mode, which was used, in particular, to align the optical system. Laser radiation entered the system via optic fiber *2*. The flexibility of the optic fiber made it possible to place the light source to any convenient location. Owing to the small diameter of the fiber, the light beam it emitted had a wide directivity pattern and therefore evenly illuminated the parabolic mirror. The phase front of the wave incident on the mirror with a high accuracy was spherical. In addition to this laser source, the setup could use a continuously working white light lamp (RAM Optical Instrumentation Inc., CA, United States). The radiation from the lamp was fed to a flexible fiberoptic bundle. A diaphragm was attached to the bundle face to decrease the effective diameter of the optical source to submillimeter size.

A point light source (one of the two abovementioned sources) was placed at the focus of the off-axis parabolic mirror. In total, the system had two flat mirrors *3* and two off-axis parabolic mirrors *4*. All of these mirrors were made of optical pyroceramics ("sitall"). The flat mirrors had a circular shape, their diameter was 158 mm, and their thickness was 25.3 mm. The off-axis parabolic mirrors were obtained as a result of cutting into two equal halves a circular axially symmetric parabolic mirror 300 mm in diameter, 30 mm thick at the edge, and 28.2 mm thick at the center. The focal length of the parabolic mirrors was 800 mm (the focal length of the initial axially symmetric mirror). The first off-axis parabolic mirror, at the focus of which the point light source was located, generated a plane-parallel beam, which was directed by the flat mirror *3* to the studied region (water tank *5*). The tank contained the ultrasound source that generated in the water spatiotemporal inhomogeneities in optical refractive index *6*. Having experienced refraction on acoustic inhomogeneities, the optical beam departed the tank. Passing further through the symmetric shoulder formed by pair of mirrors *3* and *4*, the light was collected at the focus of the second parabolic mirror, positioned symmetrically to the initial point light source. At the focal region an optical knife *7* was placed, which was a blade with a straight edge. When the knife was introduced into the focal spot region, suppression of background illumination occurred and contrast of the schlieren image was increased. After passing the knife, the light beam was directed via a deflecting mirror at the lens that formed the acoustic field image on the CCD sensor of a Kodak ES 310 8-bit digital camera *8*. Selecting the forming lens with a different optical power made it possible to observe the entire illumination region or only part of it, magnifying the image to visualize small details. Then, the digitized image was transmitted to a personal computer *9*, equipped with a card with a GPIB interface. An important property of the schlieren system was complete computerization of image processing with a program written in the LabVIEW language. This strongly enriched the image-processing capabilities. In particular, due to this, it was possible to average the image over the number of frames, which was particularly important for a low image intensity. Another capability was subtraction of the background, which

made it possible to clean the image of artifacts caused by dust particles on the optical elements, air bubbles in the water, and diffraction bands on the borders of nontransparent objects.

To measure the distances between characteristic points of the shadow pattern, we calibrated the spatial scales in the visualization zone by recording the image of a transparent millimeter ruler. With pulse illumination of the ultrasound fields of known frequency, it was possible to additionally check the calibration of scales based on the fact that the period of inhomogeneities in the shadow pattern was equal to the wavelength.

MEASUREMENT RESULTS

As mentioned above, when conducting experiments, we measured the optical shadow pattern of the ultrasound field, the caustics region in it, and distances r_c from the caustics to the center of the plate curvature; then we calculated the phase velocity by formula (2).

Illumination was made by short flashes synchronized with the electric signal fed to the transducer. Since the duration of the corresponding laser pulses (0.1 μs) in the entire range of frequencies used was much smaller than the period of an ultrasound wave (around 1 μs), the shadow pattern was the instantaneous distribution of perturbations in the density of the medium; i.e., it was possible to analyze fine details of the ultrasound field.

Figure 5 shows a typical shadow pattern (the corresponding frequency is 600 kHz). One can distinctly see the periodicity of the field structure. The corresponding period coincides with the wavelength of the ultrasound wave. To find distance r_c entering formula (2), it is necessary to know the location of the geometric focus and the caustics. The location of the geometric focus can be determined with high accuracy using the spherical character of the wave fronts in the main beam emitted as a result of thickness vibrations of the piezoelectric plate. Here, to increase the accuracy of finding the geometric focus, high frequencies can be used, since the corresponding field is not as subjected to the influence of diffraction. Note that the geometric focus coincides with the center of curvature of the plate; therefore, its location does not depend on the ultrasound frequency. The location of the caustics, in contrast, is frequency-dependent. The caustics is a geometric object determined in the geometrical acoustics approximation. In reality, at the place of the caustics, the focusing region is blurred by diffraction. Here, the amplitude of the ultrasound wave is noticeably increased in comparison to the surrounding regions; i.e., the shadow pattern is more contrasting. Observations show that these regions are quite distinctly seen in the overall shadow pattern. For instance, in Fig. 5, two such caustics can be seen: they are denoted on the right by circular arcs. The corresponding distances r_c from the found caustics to the center of curvature of the plate are denoted by segments with arrows departing from the geometric focus. As one can see, the accuracy in finding r_c is given by the width of diffraction blurring of the caustics (on the order of the wavelength of the ultrasound wave at the corresponding frequency); i.e., it can be directly estimated from the type of shadow pattern.

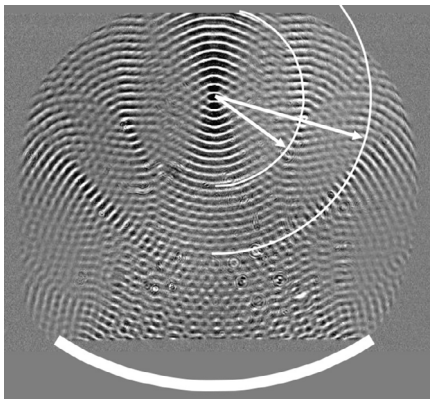

Fig. 5. Typical shadow pattern of ultrasound field emitted by focused piezoceramic source. Excitation frequency 600 kHz. Position of source shown by thick white arc in lower part of figure. Brightest region is main focus generated at center of curvature of piezoelectric plate as result of excitation of its thickness vibration mode. Along with main focus, side focal regions can be seen corresponding to caustics (shown by thin circular arcs on right-hand side of image). At the chosen frequency, two caustics are observed, which correspond to symmetric and antisymmetric lower-order Lamb modes.

The shadow patterns similar to those depicted in Fig. 5 were recorded at different frequencies. Figure 6 shows some of the obtained images. As one can see, at all frequencies, the caustics are well seen; with increasing frequency, their number increases; the location depends of the frequency.

Based on the obtained images, the phase velocities of the corresponding leaky waves were calculated by formula (2). The corresponding circumferences were chosen manually, so that the centers of the narrowest areas of caustics were on them. Note that this procedure in principle can be automated using digital optical image processing (in this work, this was not done). In Fig. 7, the results are indicated by points with the values of errors given by the size of diffraction blurring of the corresponding caustics in the thinnest part of it. Solid curves depict the dispersion dependences calculated theoretically by the Rayleigh–Lamb formulas under the assumption that the plate material is isotropic [2]. Although this assumption, strictly speaking, is violated in the case of the piezoelectric plate under study, it is possible to expect at least qualitative agreement with experiment.

Recall that Lamb waves are devided into symmetric (s_n) and antisymmetric (a_n) modes, where $n = 0$,

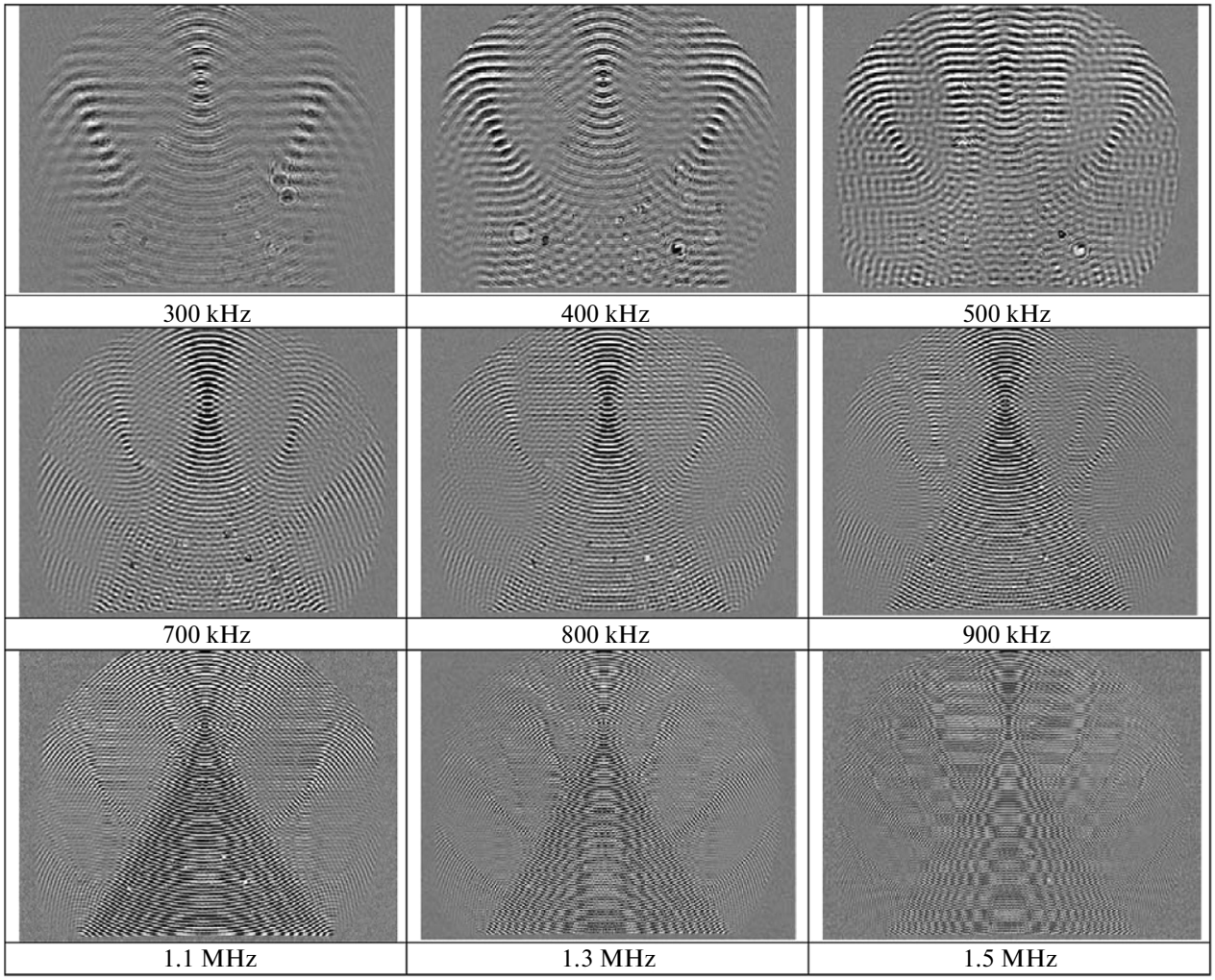

Fig. 6. Shadow pattern of ultrasound field emitted by focused piezoceramic source at different frequencies.

1, 2, ... is the mode number. At low frequencies, there are only two propagating modes, s_0 and a_0, which are a quasilongitudinal and flexural waves, respectively. In contrast to zero-order modes, higher-order modes can propagate in the plate only in the case when the excitation frequency exceeds certain critical values. When calculating the dispersion curves by the Rayleigh–Lamb formulas, we used a plate thickness of 2.15 mm and took velocities of bulk waves of c_l = 4.64 mm/μs (based on the measured value of the thickness resonance frequency) and c_t = 2.02 mm/μs (based on the observed mode cutoff frequency a_1). Figure 7 shows the dispersion curves for lower-order Lamb modes up to the second order. One can see that the theoretical curves for modes s_0, a_0, s_1, and a_1 coincide with the results of measurements within the measurement error limits. Mode a_0 begins to be observed only starting at a frequency of 700 kHz, which is explained by the fact that at lower frequencies it is "nonleaky," since the phase velocity of the corresponding Lamb wave is less that the sound velocity in water. Note also that for modes s_2 and a_2, the experiment does not coincide with the theory, which can be explained by the manifestation of anisotropy, which is not taken into account in the theoretical model.

CONCLUSIONS

The paper demonstrated the capabilities of the optical shadowgraphy method for studying the properties of Lamb waves in piezoelectric plates submerged in a fluid. The approach is based on the fact that if the phase velocity of a Lamb wave exceeds the sound velocity in a fluid, then for mechanical excitation of a piezoelectric plate, radiation of acoustic waves in the fluid occurs. The direction of propagation of these waves is unambiguously determined by the value of the phase velocity of a wave in a plate, which makes it possible to measure the indicated velocity. It is especially convenient to conduct

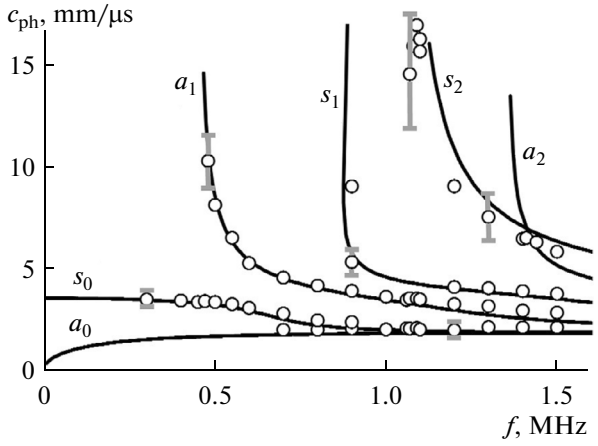

Fig. 7. Dispersion curves for different Lamb modes in piezoceramic plate. Points correspond to experimental shadow patterns. Theoretical curves are solutions to Rayleigh–Lamb equations in approximation of isotropic medium, calculated using velocity values of $c_t = 1.94$ mm/μs, found from measured a_1 mode cutoff frequencies (0.45 MHz) and thickness resonance frequency (1.08 MHz), respectively, taking into account known thickness of plate (2.15 mm).

measurements using spherically concave plates, since in this case the direction of wave propagation in a fluid determined the location of the caustics, which are distinctly seen in the shadow pattern of the ultrasound field. In the conducted experiment, the proposed method made it possible the measure the dispersion curves of lower-order Lamb modes of a concave piezoelectric plate with parameters typical of modern ultrasound sources used in medicine.

ACKNOWLEDGMENTS

The authors thank B.Yu. Terletskii for assistance in preparing the laser control block, A.E. Ponomarev for creating the program for controlling the digital camera, and V.G. Mozhaev for helpful discussion of the results.

The work was financially supported by the Russian Foundation for Basic Research (project no. 14-02-00426).

REFERENCES

1. H. Lamb, Proc. R. Soc. London, Ser. A **93**, 114 (1917).
2. I. A. Viktorov, *Physical Foundations of Rayleigh and Lamb Ultrasound Waves in Technics* (Nauka, Moscow, 1966) [in Russian].
3. L. M. Brekhovskikh, *Waves in Layered Media* (Academic, New York, 1960; Nauka, Moscow, 1973).
4. R. D. Watkins, W. H. B. Cooper, A. B. Gillespie, and R. B. Pike, Ultrasonics **20**, 257 (1982).
5. I. E. Kuznetsova, B. D. Zaitsev, S. G. Dzhoshi, and A. A. Teplykh, Acoust. Phys. **53**, 637 (2007).
6. J. C. Baboux, F. Lakestani, and M. Perdrix, J. Acoust. Soc. Am. **75**, 1722 (1984).
7. X. Jia, J. Berger, and G. Quentin, J. Acoust. Soc. Am. **90**, 1181 (1991).
8. B. Delannoy, C. Bruneel, F. Haine, and R. Torguet, J. Appl. Phys. **51**, 3942 (1980).
9. D. Cathignol, O. A. Sapozhnikov, and J. Zhang, J. Acoust. Soc. Am. **101**, 1286 (1997).
10. D. Cathignol, O. A. Sapozhnikov, and Y. Theillere, J. Acoust. Soc. Am. **105**, 2612 (1999).
11. M. S. Canney, M. R. Bailey, L. A. Crum, V. A. Khokhlova, and O. A. Sapozhnikov, J. Acoust. Soc. Am. **124**, 2406 (2008).
12. O. A. Sapozhnikov, Yu. A. Pishchal'nikov, and A. V. Morozov, Acoust. Phys. **49**, 354 (2003).
13. S. V. Kuznetsov, Acoust. Phys. **60**, 95 (2014).
14. Yu. P. Gaidukov, N. P. Danilova, and O. A. Sapozhnikov, Acoust. Phys. **45**, 163 (1999).
15. G. S. Settles, *Schlieren and Shadowgraph Techniques: Visualizing Phenomena in Transparent Media* (Springer-Verlag, 2001).
16. L. Bergman, *Ultrasound and Its Applications in Acoustics* (InLit, Moscow, 1956) [in Russian].
17. Yu. M. Kuz'michev and V. I. Makarov, Akust. Zh. **4**, 282 (1958).
18. V. I. Makarov and N. A. Fadeeva, Akust. Zh. **6**, 261 (1960).

Translated by A. Carpenter